



## **EFFECT OF REDUCED SUCTION SIDE VOLUME ON CROSS-FLOW FAN PERFORMANCE**

Matteo SPINOLA<sup>1</sup>, Paolo GOBBATO<sup>1</sup>,  
Andrea LAZZARETTO<sup>1</sup>, Massimo MASI<sup>2</sup>

<sup>1</sup> *Department of Industrial Engineering, University of Padova,  
via Venezia, 1 – 35131 Padova, Italy*

<sup>2</sup> *Department of Management and Engineering, University of Padova,  
stradella S. Nicola, 3 – 36100 Vicenza, Italy*

### *SUMMARY*

In most of the high-performance cross-flow fans appeared in the literature the position of the vortex wall and the shape of the casing rear wall yield an approximately ninety degrees air flow deflection between inlet and outlet sides. However, industrial applications may require different layouts due to physical constraints which limit the radial width of the fan, and there are very few studies in the literature that deal with similar restrictions. This paper presents the results of experimental tests aimed at investigating the effect of suction side volume limitation on the performance of a small cross-flow fan. Results may support fan design choices when the application imposes limited operating volumes.

### **INTRODUCTION**

Cross-flow fans are widely used in industrial and domestic applications in which the radial space availability for fan operation is limited. Unlike other type of fans, the cross-flow fan internal flow field is characterised by an eccentric vortex resulting from blades circulation, which forces the flow to be worked out two times by the rotor blades. Due to the vortex formation, a rotating cross-flow impeller generates a non-symmetrical throughflow, also when operates in unbounded fluid. In particular, the inlet flow is deflected of about 90 degrees by the impeller, as determined in early visualization studies [1]. This natural arrangement of the flow is achieved also in high-performance cross-flow fans in the literature [1-9], in which a vortex wall and a rear wall guide the flow through the impeller (as sketched in Fig. 1). For this layout, the set of independent design parameters most affecting fan performance [10], and their isolated effect on fan performance [9] and on the internal flow field [11] seem to be well established. An objective-dependent design guidelines were also proposed in [12] by the same authors. On the basis of these studies, it can be deduced that a cross-flow fan shows the best performance when its suction side is not limited along the radial direction. This evidence will be confirmed by the results of the present work.

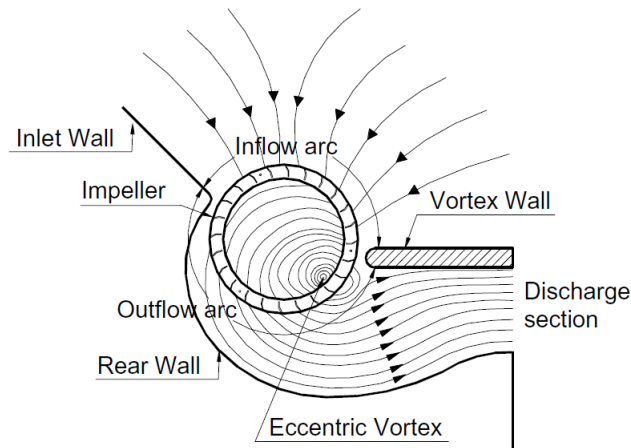


Figure 1: Typical arrangement of the flow field with a bounded-fluid cross-flow fan.

However, applications in ventilation/air conditioning, aircraft propulsion and automotive systems may require different layouts due to physical constraints which limit the radial width of the fan and reduce its suction side volume.

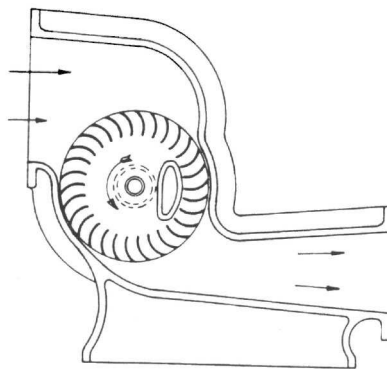


Figure 2: Mortier's cross-flow fan (taken from [13]).

In 1892 Mortier got a patent for the invention of the cross-flow fan to be applied in mine ventilation [13]. In the configuration he proposed, the inlet flow is guided through the impeller by means of a duct parallel to the discharge duct (Fig. 2). To achieve a parallel arrangement between inlet and outlet flows, the suction side is limited along the radial direction. Unfortunately, the inventor did not provide any performance of such configuration and, to the knowledge of the present authors, no other documents of the literature deal with similar restriction of the inlet side.

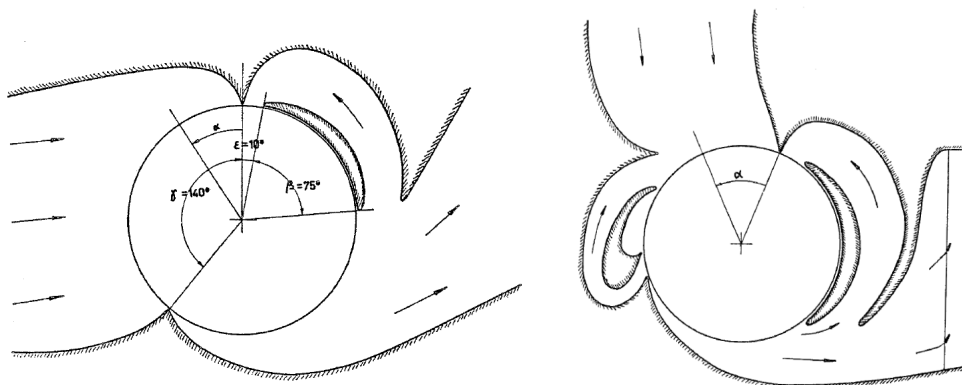


Figure 3: Two of Coester's cross-flow fan configurations (taken from [14]).

The only study that is worth being mentioned was carried out by Coester [14]. In the study the author presented the results of experimental tests of several complex configurations (such as those shown in Fig. 3). However, the analysed fans feature very short impellers ( $L/D_2 \approx 0.1$ ) and were tested at high rotational speeds (up to 15000 rpm). Consequently Coester's conclusions may not be useful to outline the performance of typical impeller aspect ratios and operating conditions.

In the present work, the effect of the suction side volume limitation along the radial direction on the performance of a small cross-flow impeller is experimentally investigated. A baseline fan configuration is chosen among several configurations featuring different rear wall shapes and vortex wall positions because of its best trade-off between efficiency, maximum flow rate, pressure rise and stability of the performance curve. Two sets of tests were performed by modifying this baseline configuration. In the first set, the effect of the inlet wall size (see Fig. 1) was investigated. Then, the suction side was constrained by using a flat plate parallel to the outlet flow direction to achieve an in-line flow layout. The flat plate was gradually moved to reduce the available volume at the suction side. Fan performance was measured for each position of the flat plate to evaluate the performance reduction with respect to the baseline configuration.

## EXPERIMENTAL APPARATUS AND TEST PLAN

The test apparatus is the same used in [9,11,15], which was built according to the ISO 5801 [16] standard on industrial fans test methods and acceptance conditions. The facility, schematically shown in Fig. 4, is of category A “free inlet – free outlet”, featuring a standardised outlet test chamber.

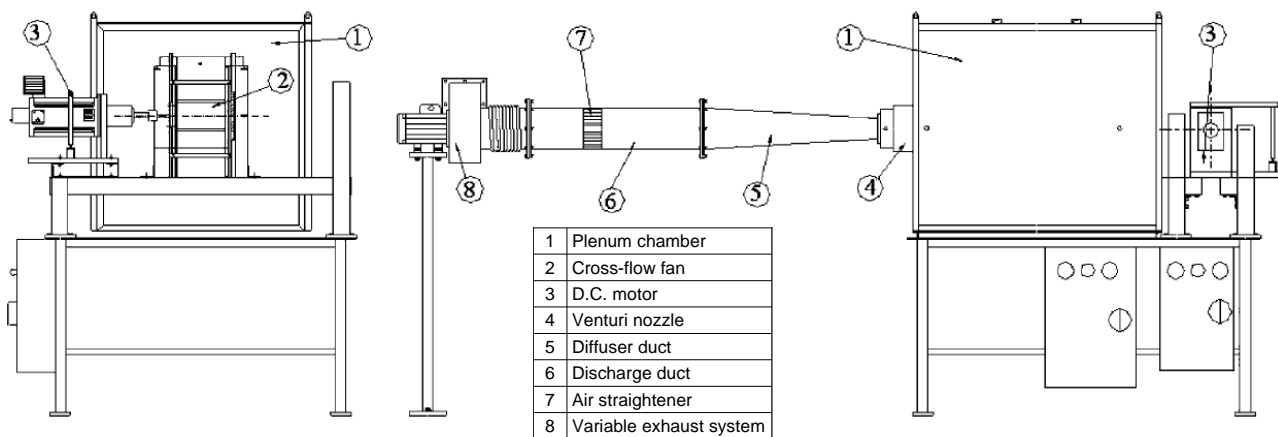


Figure 4: Schematic of the test rig.

A Venturi nozzle is positioned at the outlet of the plenum chamber to measure the mass flow rate. At the end of the airway, after a honeycomb straightener, an auxiliary fan is placed to overcome the pressure losses of the test rig. Static pressure measurements of the chamber and nozzle tappings are taken using water micromanometers having 1/100 mm H<sub>2</sub>O accuracy. The D.C. motor driving the fan includes a tachometric dynamo for rotational speed measurements. A load cell (range  $\pm 0.5$  kg, sensitivity 16 mV/V and accuracy  $\pm 1$  %) connected to the motor stator by means of a lever arm is used for torque measurement to determine the fan total efficiency. The power absorbed by bearings and winding was evaluated by running a bladeless impeller having the same moment of inertia as the actual one.

All tests were conducted, when possible, at a rotational speed of 1000 rpm. Accordingly, the fan is operating at a blade Reynolds number approximately  $Re_b=7600$ , which is above the 6000–7000 threshold recommended by Lazzarotto et al. [15] to meet similarity conditions. However, at high

flow rates ( $\phi > 1$ ), the auxiliary fan showed to be unable to overcome all the pressure losses in the airway, requiring a gradual reduction of the fan speed to 650 rpm. The similarity of operations was therefore not met in test points with  $\phi > 1$ , which means that the real performance in that range of the tested fans may be higher than the values provided.

In each test, the curves of total pressure coefficient  $\psi_t$  and total efficiency  $\eta_t$  versus flow coefficient  $\phi$  are plotted in agreement with the following definitions:

$$\psi_t = \frac{P_t}{0.5\rho u_2^2}; \quad \phi = \frac{q}{u_2 D_2 L}; \quad \eta_t = \frac{P_t q}{P} \quad (1)$$

Where  $p_t$  is the fan total pressure,  $\rho$  is the air density,  $u_2$  is the fan peripheral speed,  $q$  is the volumetric flow rate and  $P$  is the mechanical power at the fan shaft. Experimental data points were acquired from zero flow rate to free delivery (zero back pressure at fan discharge).

### Impeller geometry

The cross-flow fan impeller used in the tests features an external diameter  $D_2$  of 152.4 mm, an axial length  $L$  of 228.6 mm ( $L/D_2=1.5$ ), a number of blades of  $Z = 24$  and a diameter ratio of  $D_1/D_2=0.81$  (Fig. 5). The internal and external blade angles of the impeller ( $\beta_1$  and  $\beta_2$ ) equals  $90^\circ$  and  $25^\circ$ , respectively, and the blade thickness  $s_b$  is 2 mm. This impeller was chosen among other available impellers because of the high performance and efficiency shown in previous tests [11,12].

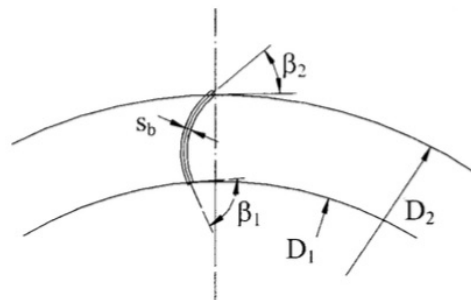


Figure 5: Impeller design parameters.

### Baseline configuration

The baseline configuration is named "R2r-H1" in [9, 11, 12, 15] and it is sketched in Fig. 6. It features a logarithmic spiral rear wall (R2r) of intermediate depth ( $\theta^*=191^\circ$ ) with a straight discharge duct and a flat and thin vortex wall located in the lowest position of Fig. 6 (H1). The suction side of the baseline configuration was modified to obtain several new configurations, as explained in the following Section.

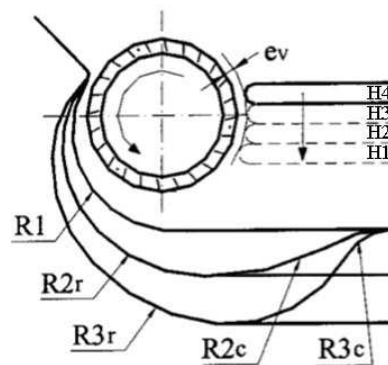


Figure 6: Baseline configuration with different shapes of the rear wall (R1 to R3c) and positions of the vortex wall (H1 to H4). The R2r-H1 is the configuration tested.

### Test plan

In the baseline configuration, the inflow arc is azimuthally limited in the throughflow plane by a tilted inlet wall, the test chamber casing and the vortex wall (Fig. 7). The size of the inlet wall greatly affects the space occupied by the fan in the throughflow plane, as clearly visible in the same figure. Thus, it is interesting to investigate the influence of this inlet wall on fan performance and efficiency. A first series of tests was performed on five open-inlet configurations that were obtained by progressively cutting the inlet wall along the dashed lines shown in Fig. 7. The resulting configurations are listed in the legend of Fig. 7 and identified by the letter "I" followed by a number, which indicates the dimensionless inlet wall size ( $h_I/D_2$ ).

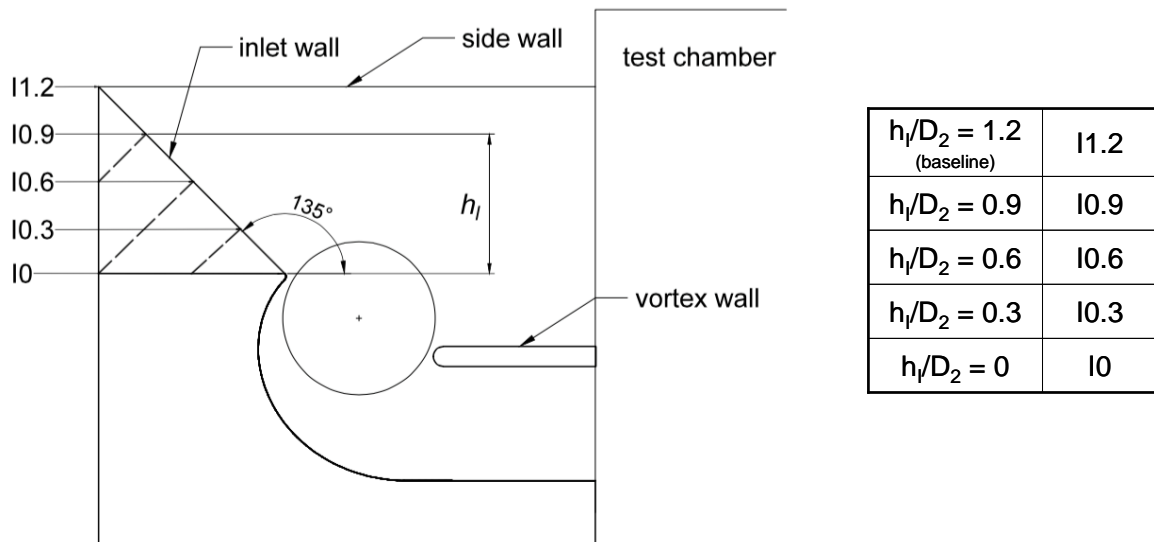


Figure 7: Open-inlet configurations featured by five inlet wall sizes ( $h_I/D_2=1.2, 0.9, 0.6, 0.3,$  and  $0$ ).

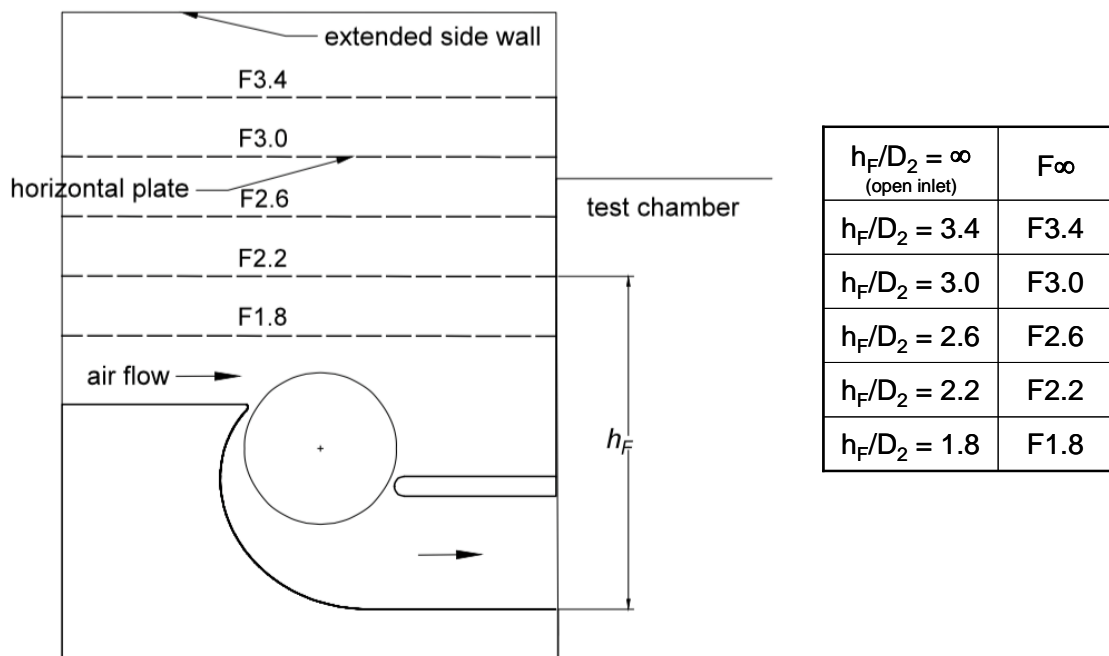


Figure 8: Configurations obtained by moving the horizontal plate to five different positions ( $h_F/D_2=3.4, 3.0, 2.6, 2.2$  and  $1.8$ ). The figure shows the  $h_I/D_2=0$  inlet wall size.

In the second series of tests, a flat, horizontal plate was interposed between the casing side walls to reduce the suction side volume available to the fan (Fig. 8). As a consequence, the usual  $90^\circ$

deflection of the fan throughflow is forced to be  $0^\circ$  (i.e., inlet flow parallel to the outlet flow). Being the radial depth of the rear wall fixed, the total height of the fan  $h_F$  is chosen as parameter to identify the position of the horizontal plate and, as a result, the size of the suction side volume.

The test rig of Fig. 7 was modified by extending the side walls upwards to support the plate in five different positions. The configurations tested are identified by the letter "F" followed by a number, which indicates the  $h_F/D_2$  ratio (the open-inlet configurations feature an infinite value of  $h_F/D_2$  ratio and are consequently identified by the notation  $F_\infty$ ).

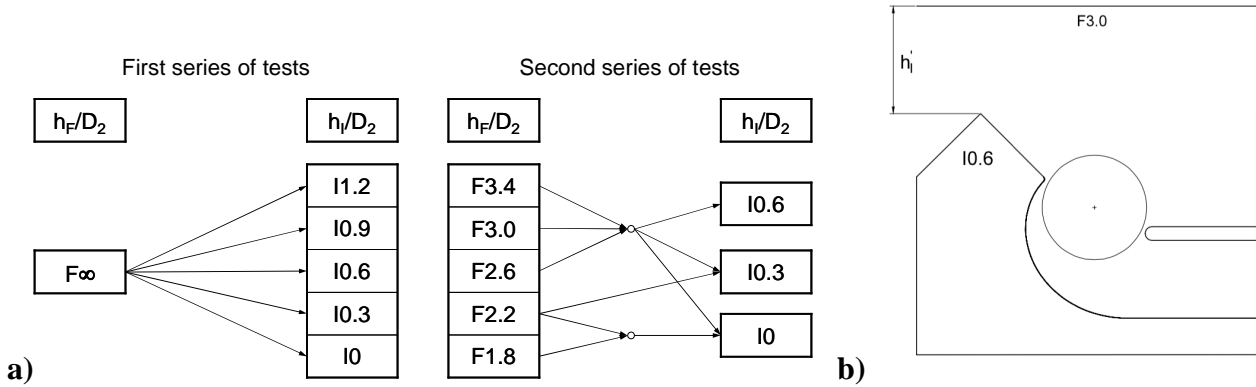


Figure 9: Fan configurations considered in the experimental tests (a) and F3.0-I0.6 configuration (b).

Figure 9a collects all the fan configurations tested (5 in the first series and 12 in the second series). Note that, in the second series, only the 10, 10.3 and 10.6 inlet wall sizes were considered to focus the attention on reduced inlet volume configurations. Moreover, not all the five positions of the horizontal plate (column on left side) were tested in combination with each size of the inlet wall (column on right side) because of the very narrow height of the fan inlet section ( $h_I$  in Fig. 9b), which causes an unacceptable performance drop. Figure 9b shows one of the configurations tested (F0.3-I0.6) during the second series of tests.

## RESULTS

### First test series: effect of the inlet wall size in the open-inlet fan configuration

The dimensionless performance curves of the open-inlet configurations (see Fig. 7) at different  $h_I/D_2$  ratios (10, 10.3, 10.6, 10.9 and 11.2) are plotted in Fig. 10. The size of the inlet wall has a slight impact on both fan total pressure coefficient and efficiency over the whole operating range.

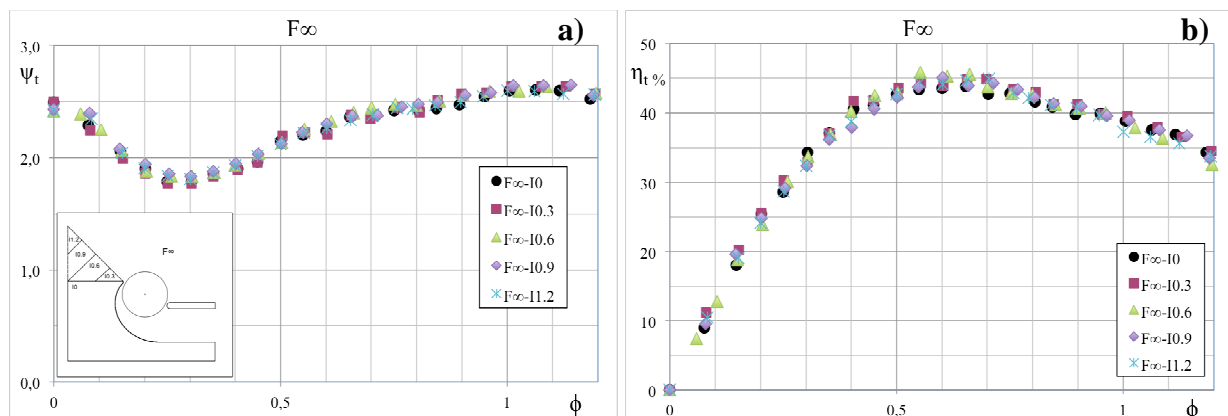


Figure 10: Effect of the inlet wall size on fan total pressure coefficient (a) and total efficiency (b). Values for open-inlet configurations ( $F_\infty$ ).

This evidence is consistent with the structure of the flow field at the fan suction side (Fig. 11). In fact, the inlet wall (red dashed triangle in the figure) is located at the opposite side of the effective suction arc, which is likely to be almost unaffected by the inlet wall size.

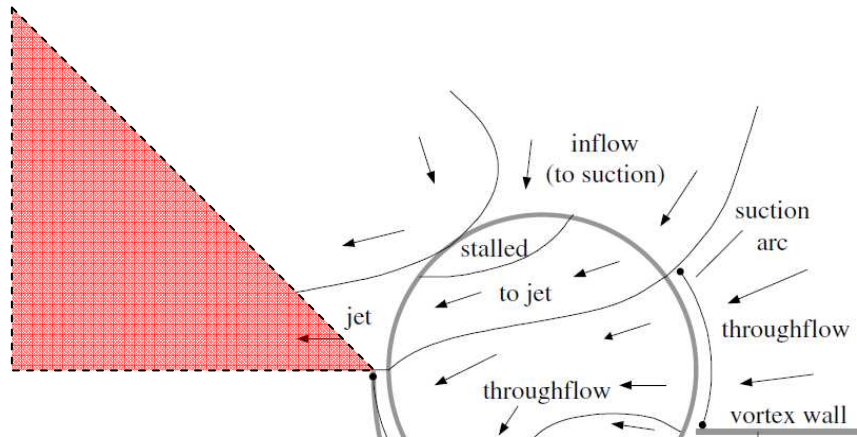


Figure 11: Regions of the flow field in a cross-flow fan (adapted from [11]).

### Second test series: reduction of the suction side volume

The results of the second series of tests are collected in Figs. 12 to 14. Figures 12a-12d show the performance curves for four positions of the horizontal plate  $h_F/D_2$  (configurations F3.4, F3.0, F2.6 and F2.2, respectively). In each graph the curves are plotted for different sizes of the inlet wall,  $h_I/D_2$  (I0, I0.3 and I0.6). Results of the F1.8 configuration are not included in Fig. 12 because the fan was not able to produce any measurable throughflow.

Figure 12 clearly shows that the reduction of the suction side volume causes a notable decrease of fan performance. Moreover, the effect of the inlet wall size on both fan pressure coefficient and total efficiency is more significant than in the open-inlet configurations (compare Figs. 12a and 12b with Fig. 10).

A slight confinement of the inlet flow (F3.4, Fig. 12a) causes a limited decrease of both the open-inlet configuration efficiency and total pressure coefficient. Performance is further reduced by the F3 configuration (Fig. 12b) and strongly worsen by the F2.6 and F2.2 configurations where the plate is very close to the impeller. When the inlet volume is very limited (F2.2, Fig. 12d) the inlet wall should be removed (I0 configuration).

Experimental data in Fig. 12 are rearranged in Fig. 13 to further investigate the decrease of fan performance due to a reduction of the suction side volume. The main outcomes are listed in the following:

- As expected, the best configurations are the open-inlet ones ( $F_\infty$ ). Among these configurations, the I0.6 inlet wall size leads to the highest maximum efficiency.
- The maximum fan flow rate decreases moving the plate towards the impeller (from  $F_\infty$  to F2.6). The gradual decrease becomes sudden when the plate is very close to the impeller (configurations F2.2 and partly F2.6).
- Pressure and efficiency peak flow coefficients decrease when the suction side volume decreases.
- In F2.6-I0.6, F2.2-I0.3 and F2.2-I0 configurations fan total pressure coefficient is apparently penalised for flow coefficients higher than 0.3.

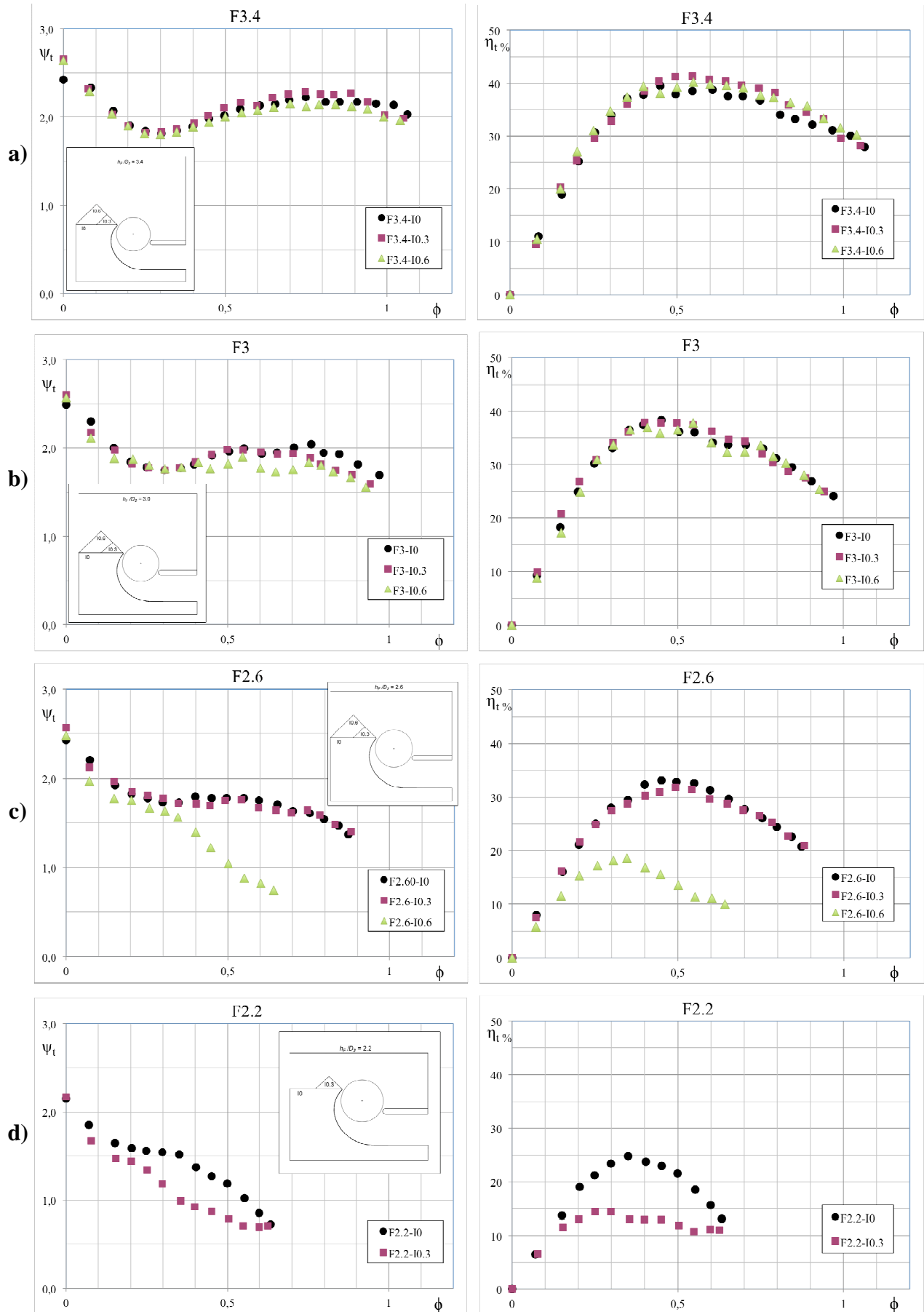


Figure 12: Effect of the inlet wall size on fan total pressure coefficient (left) and total efficiency (right) for different positions of the horizontal plate (F3.4, F3.0, F2.6 and F2.2).



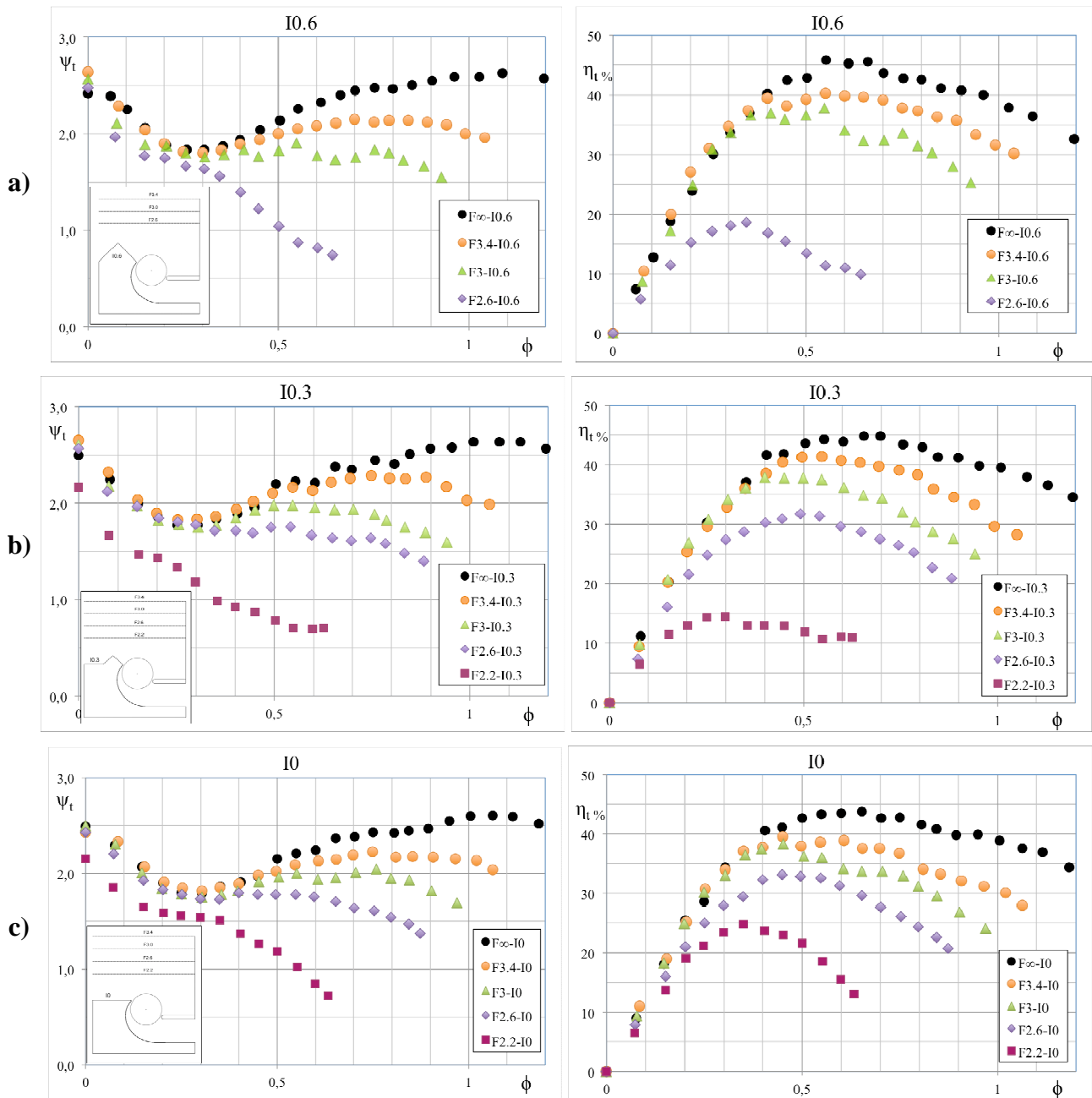


Figure 13: Effect of the horizontal plate position on fan total pressure coefficient (left) and total efficiency (right) for decreasing size of the inlet wall (IO.6, IO.3 and IO) from a) to c).

Results shown in Figs. 12 and 13 suggest to consider another design variable, the height of the fan inlet section ( $h'_I$  in Fig. 9b), which depends on both the size of the inlet wall ( $h_I$ ) and position of the horizontal plate ( $h_F$ , see Figs. 7 and 8). The characteristic curves corresponding to  $h'_I/D_2$  values derived from the tested fan configurations are plotted in Fig. 14 (for sake of convenience the  $h'_I/D_2$  ratios are abbreviated with "I" in the same figure). It can be noted that for confined configurations ( $h_F/D_2 < \infty$ ) a wider inlet section does not necessary lead to higher pressure and efficiency. For medium-to-high height of the inlet section ( $h'_I/D_2 > 0.95$ ) the fan performs better if the incoming flow is guided by the inlet wall (IO.3 and IO.6 configurations). This implies that the inlet section height  $h'_I$  is not able to combine the effect of inlet wall ( $h_I$ ) and position of the horizontal plate ( $h_F$ ) on fan performance.

Furthermore, it is clear that, for medium-to-high flow rates ( $\phi > 0.3$ ), fan configurations featuring narrow inlet sections ( $h'_I/D_2$  ratio between 0.55 and 0.85) performed noticeably worse than all other configurations. In other words, a critical value of the inlet section height exists, below which the fan

performance drops significantly. For the tested cross-flow fan this value ranges between 0.85 and 0.95. Over  $h'/D_2=0.95$  the improvement in fan performance is not so pronounced.

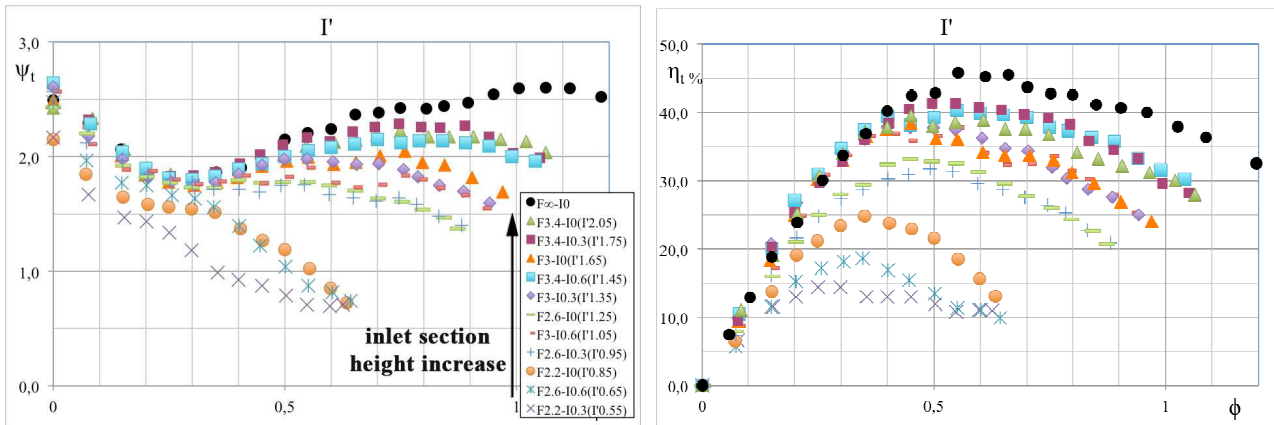


Figure 14: Effect of the inlet section height ( $h'/D_2$  abbreviated with  $I'$ ) on fan total pressure coefficient (left) and total efficiency (right).  $F_{\infty}$  denotes the open-inlet configuration.

## CONCLUSIONS

An experimental test program was carried out to investigate the effect of the limitation of the suction side volume on the performance of a cross-flow fan. A reduction of the inlet volume may be necessary in several applications where the space available for the fan operation is limited.

A baseline fan configuration is chosen to be modified and tested over a wide range of mass flow rates. Two series of test were carried out. In the first series, the effect of the inlet wall size was investigated for an open-inlet configuration. This because the inlet wall noticeable contributes to the total radial size of the fan. In the second series of tests, the suction side was constrained by using a flat plate parallel to the outlet flow direction to achieve an in-line flow layout. The flat plate was gradually moved to reduce the available suction side volume.

Results of first series of tests show that the size of the inlet wall does not significantly affect both fan pressure coefficient and efficiency.

The second series of tests quantified the decrease of fan performance due to reduction of the suction side volume. In particular, fan total pressure and total efficiency strongly drop when the horizontal plate is very close to the impeller. Measured values show also that both peak pressure and best efficiency flow coefficients decrease as the inlet volume is progressively reduced.

Experimental data were also rearranged to analyse the effect of the inlet section height on the fan performance. A critical value between 0.85 and 0.95 of this variable was identified below which the fan performance decreases significantly. However, the inlet section height cannot completely include the effect of  $h_I$  and  $h_F$  design parameters.

In summary, the experimental tests showed that the position of the horizontal plate (i.e., the design parameter which mostly affects the extension of the suction side volume) is also the parameter that most affects fan performance, whereas the inlet wall size may lead to slight performance improvements only in confined configurations.

## NOMENCLATURE

$D$  = diameter (m)

$h$  = height (m)

$L$  = impeller axial length (m)

$n$  = rotational speed (rpm)

$p$  = pressure (Pa)

$P$  = power (W)

$q$  = volumetric flow rate (m<sup>3</sup>/s)

$R$  = radial coordinate of the rear wall logarithmic spiral arc (m)

$R_0$  = starting radius of the rear wall logarithmic spiral arc (m)

$Re$  = Reynolds number

$s$  = thickness (m)

$u$  = peripheral speed (m/s)

$Z$  = number of blades

### Greek

$\beta$  = blade angle (deg)

$\eta$  = efficiency

$\theta$  = radial coordinate of the rear wall logarithmic spiral arc (deg)

$\theta^*$  = angle which defines the radial width of the rear wall according to the logarithmic spiral law,

$$R = R_0 \cdot e^{\theta/\theta^*} \text{ (deg)}$$

$\phi$  = flow coefficient

$\rho$  = air density (kg/m<sup>3</sup>)

$\psi$  = pressure coefficient

### Subscripts

1 = internal

2 = external

$b$  = blade

$t$  = total

$I$  = inlet

$F$  = fan

$R$  = rear wall

$V$  = vortex wall

## BIBLIOGRAPHY

- [1] K. Yamafuji – *Studies on the flow of cross-flow impellers - 1st report, experimental study*, Bulletin of the JSME 18(123):1018– 1025, **1975**
- [2] A.M. Porter, E. Markland – *A study of the cross flow fan*, J. Mech. Eng. Sci. 12(6):421–431, **1970**
- [3] S. Murata, K. Nishihara – *An experimental study of cross flow fan (1st report, effects of housing geometry on the fan performance)*, Bulletin of the JSME 19(129):314–321, **1976**
- [4] S. Murata, K. Nishihara – *An experimental study of cross flow fan (2nd report, movements of eccentric vortex inside impeller)*, Bulletin of the JSME 19(129):322–329, **1976**
- [5] B. Eck – *Fans*, Oxford: Pergamon Press, **1973**
- [6] D.J. Allen – *The effect of rotor and casing design on cross-flow fan performance*, In International conference on fan design and applications. Guilford, England, Paper no. J1, **1982**
- [7] H. Trampusch – *Cross-flow fan*, ASME Paper no. 64-WA/FE-25, **1964**
- [8] L. Preszler, T. Lajos – *Experiments for the development of the tangential flow fan*, In Proc. Fourth Conf. Fluid Machinery, Akadémiai Kiadó, Budapest, pp. 1071–1082, **1972**
- [9] A. Lazzaretto, A. Toffolo, A.D. Martegani – *A systematic experimental approach to cross-flow fan design*, J. Fluids Eng. 125:680–3, **2003**
- [10] A. Lazzaretto – *A criterion to define cross-flow fan design parameters*, J. Fluids Eng. 125:684–93, **2003**
- [11] A. Toffolo, A. Lazzaretto, A.D. Martegani – *An experimental investigation of the flow field pattern within the impeller of a cross-flow fan*, Exp. Therm. Fluid Sci. 29(1):53–64, **2004**
- [12] A. Toffolo, A. Lazzaretto, A.D. Martegani – *Cross-flow fan design guidelines for multi-objective performance optimization*, Proceedings of the Institution of Mechanical Engineers, Part A: J. Power En. 218(1):33–42, **2004**
- [13] P. Mortier – *Fan or blowing apparatus*, US Patent 507 445, **1893**
- [14] R. Coester – *Theoretische und experimentelle Untersuchungen an Querstromgebläsen*, vol. 28, Zürich: Mitt Inst für Aerodyn, **1959**
- [15] L. Lazzarotto, A. Lazzaretto, A. Macor, A.D. Martegani – *On cross-flow fan similarity: effects of casing shape*, J. Fluids Eng. 123(3):523–31, **2001**
- [16] ISO 5801 – *Industrial fans - performance testing using standardized airways*, **2008**